Modern Pathology (2021) 34:1530–1540
https://doi.org/10.1038/s41379-021-00806-w

ARTICLE

Novel *BRAF* gene fusions and activating point mutations in spindle cell sarcomas with histologic overlap with infantile fibrosarcoma

Alyssa J. Penning[1] · Alyaa Al-Ibraheemi[2] · Michael Michal[3,4] · Brandon T. Larsen[5] · Soo-Jin Cho[6] · Christina M. Lockwood[7] · Vera A. Paulson[7] · Yajuan J. Liu[7] · Lukáš Plank[8] · Karen Fritchie[9] · Carol Beadling[10] · Tanaya L. Neff[10] · Christopher L. Corless[1,10] · Erin R. Rudzinski[11] · Jessica L. Davis[1,10]

Received: 24 January 2021 / Revised: 23 March 2021 / Accepted: 23 March 2021 / Published online: 13 April 2021

Abstract

Infantile fibrosarcoma (IFS)/cellular congenital mesoblastic nephroma (cCMN) commonly harbors the classic *ETV6-NTRK3* translocation. However, there are recent reports of mesenchymal tumors with IFS-like morphology harboring fusions of other receptor tyrosine kinases or downstream effectors, including *NTRK1/2/3*, *MET*, *RET*, and *RAF1* fusions as well as one prior series with *BRAF* fusions. Discovery of these additional molecular drivers contributes to a more integrated diagnostic approach and presents important targets for therapy. Here we report the clinicopathologic and molecular features of 14 *BRAF*-altered tumors, of which 5 had *BRAF* point mutations and 10 harbored one or more *BRAF* fusions. Of the *BRAF* fusion-positive tumors, one harbored two *BRAF* fusions (*FOXN3-BRAF*, *TRIP11-BRAF*) and another harbored three unique alternative splice variants of *EPB41L2-BRAF*. Tumors occurred in ten males and four females, aged from birth to 32 years (median 6 months). Twelve were soft tissue based; two were visceral including one located in the kidney (cCMN). All neoplasms demonstrated ovoid to short spindle cells most frequently arranged haphazardly or in intersecting fascicles, often with collagenized stroma and a chronic inflammatory infiltrate. No specific immunophenotype was observed; expression of CD34, S100, and SMA was variable. To date, this is the largest cohort of *BRAF*-altered spindle cell neoplasms with IFS-like morphology, including not only seven novel *BRAF* fusion partners but also the first description of oncogenic *BRAF* point mutations in these tumors.

Introduction

Fibroblastic/myofibroblastic neoplasms that were once defined by morphology are increasingly being subclassified by the addition of molecular signatures, many of which are important biologic/therapeutic targets. This concept is highlighted well by the history of infantile fibrosarcoma (IFS), the most common sarcoma of infancy. First recognized and classified as a unique entity by its morphologic features [1, 2], this neoplasm was later recognized to harbor

✉ Jessica L. Davis
davisjes@ohsu.edu

1 Department of Pathology, Oregon Health & Science University, Portland, OR, USA

2 Department of Pathology, Boston Children's Hospital and Harvard Medical School, Boston, MA, USA

3 Department of Pathology, Bioptical Laboratory, Ltd., Plzen, Czech Republic

4 Department Pathology, Faculty of Medicine, Charles University, Plzen, Czech Republic

5 Department of Laboratory Medicine and Pathology, Mayo Clinic, Scottsdale, AZ, USA

6 Department of Pathology, University of California San Francisco, San Francisco, CA, USA

7 Department of Laboratory Medicine and Pathology, School of Medicine, University of Washington, Seattle, WA, USA

8 Department of Pathology, Faculty of Medicine, Comenius University Jessenius Medical Faculty, Bratislava, Czech Republic

9 Department of Pathology, Cleveland Clinic, Cleveland, OH, USA

10 Knight Cancer Institute, Oregon Health & Science University, Portland, OR, USA

11 Department of Laboratories, Seattle Children's Hospital, Seattle, WA, USA

nonrandom chromosomal gains [3, 4]. In 1998, IFS and its renal counterpart cellular congenital mesoblastic nephroma (cCMN) were found to harbor the fusion *ETV6-NTRK3* [5, 6]. Further studies have established that *ETV6-NTRK3* fusions are found in approximately 70% of IFS [7–11]. *ETV6-NTRK3* fusion-negative spindle cell soft tissue sarcomas with morphologic features overlapping with those of IFS have been observed in both the pediatric and adult populations [8–16]. It is now recognized that tumors with morphologic features of IFS may contain fusions involving other genes involved in the mitogen-activated protein kinase (MAPK) pathway, including those with *NTRK1/2* or variant *NTRK3* fusions, fusions involving *MET* or *RET*, or alterations in genes encoding downstream effector molecules such as *RAF1* (*CRAF*) and *BRAF* [8–16]. Many of these molecular alterations are targetable by novel therapies, resulting in clinical benefit in patients diagnosed with IFS-like spindle cell sarcomas harboring such alterations [13, 17–22]. Given the expanding molecular landscape of these tumors and the increasing availability of targeted therapies, identification of these molecular alterations is critical, but the spectrum of clinical, pathologic, and genetic features of this class of tumors remains poorly understood. Here we report the spectrum of activating *BRAF* alterations in a cohort of IFS-like spindle cell sarcomas, with accompanying clinicopathologic demographics, morphology, immunophenotype, and clinical outcomes.

Materials and methods

Index cases and patient selection

Two index cases were identified as part of a previously published research study examining pediatric "*ETV6* negative" tumors with morphology in the spectrum of that seen in IFS [8]. The prior study focused on *NTRK*-rearranged tumors only; of 36 cases evaluated, 6 cases were published but excluded from further clinicopathologic evaluation either because they had insufficient material for molecular analysis or the tumor did not contain *NTRK* gene alterations; 2 of those 6 cases harbored *BRAF* gene alterations [8].

Case 1 presented congenitally, with intrauterine fetal demise (IUFD) at 29-week gestation of a male fetus with an 8 cm paraspinal mass. The tumor showed a predominantly spindled cell morphology arranged in fascicles with numerous ectatic, "hemangiopericytoma (HPC)-like" vessels; admixed were areas with a cellular ovoid to round-cell morphology. Rare foci of heterologous cartilage were present. By immunohistochemistry, the tumor expressed S100 and patchy SMA, without co-expression of CD34. Florescence in situ hybridization (FISH) was negative for *ETV6* gene rearrangement, and a diagnosis of undifferentiated spindle cell sarcoma was made. Next-generation sequencing (NGS) was performed that demonstrated a likely oncogenic BRAF p.L485F substitution and *BRAF-ADCK2* fusion; no other alterations were present (Table 1).

Case 2 was a 9-day-old boy with a perirectal mass that invaded through the intestinal wall to focally involve the mucosa. Morphologically, the tumor was a cellular spindle cell neoplasm with prominent ectatic vessels; immunohistochemical stains showed diffuse SMA with patchy S100 and weak focal CD34 expression. Given concern for IFS, FISH was performed for *ETV6* rearrangement, which was negative; however, trisomy 11 was detected via karyotyping. A diagnosis of undifferentiated spindle cell sarcoma was rendered. NGS was performed that showed an activating *BRAF* p.V600D mutation; no other fusions or point mutations were present (Table 1).

Based on increased recognition of variant *NTRK* and other RTK/MAPK pathway gene fusions, morphologically similar primitive spindle cell tumors are routinely sequenced as part of clinical practice. Prompted by the results of the two index cases summarized above, a search for additional cases harboring molecular alterations in the *BRAF* gene was undertaken. An additional 12 cases with activating *BRAF* gene alterations were identified. Two pathologists (JLD and AJP) evaluated the clinicopathologic features of these *BRAF*-altered tumors.

Immunohistochemistry

Not all cases had material available for staining. A panel of IHC antibodies including CD34, S100, SMA, and Pan-Trk was applied when formalin-fixed paraffin-embedded (FFPE) tissue was available. Immunohistochemistry was performed on 4-μm paraffin-embedded whole tissue sections using standard techniques. Detection and staining for all cases was performed using a fully automated DAB antigen retrieval system (Benchmark ULTRA; Ventana Medical Systems, Tucson, AZ, USA), with appropriate controls. The following antibodies were used: mouse monoclonal anti-CD34 antibody (MU-236-4C, 1:30 dilution; BioGenex, Fremont, CA, USA), rabbit polyclonal anti-S100 (Z0311, 1:800 dilution; Dako, Santa Clara, CA, USA), mouse monoclonal anti-smooth muscle actin antibody (M085101, 1:200; Dako), and rabbit monoclonal anti-Pan-Trk antibody (EPR17341, 1:25; Abcam, Cambridge, MA, USA). The threshold for designating positivity was expression in >5% of cells.

Targeted DNA sequencing with RNA or DNA sequencing for fusion detection

DNA and RNA were extracted from FFPE tissue using standard techniques. Clinically validated targeted NGS was

Table 1 Clinicopathologic features.

Case	Age	Sex	Site	Genetics	IHC				Mits	Treatment	Mets	Outcome	Follow-up (mo)
					CD34	*S100*	*SMA*	*Pan-Trk*					
1	Congenital	M	Paraspinal	BRAF p.L485F; *BRAF-ADCK2*	–	+	Focal+	–	N/A	N/A	N/A	IUFD at 29 WGA	N/A
2	9 days	M	Perirectal/ submucosal	BRAF p.V600D	Patchy+	Patchy+	–	–	10	UNK	UNK	UNK	UNK
3	9 months	F	Neck	BRAF p.V600E	+	–	UNK	Equivocal	1	Resection	NO	NED	6
4	1 year	M	Leg	BRAF p.V600E	–	–	–	–	2	TBD	UNK	UNK	UNK
5	18 months	F	Kidney (cCMN)	BRAF p.V600E	–	Patchy+	–	–	3	Resection	NO	NED	24
6	Congenital	M	Scalp	*EPB41L2-BRAF*[a]	Focal+	Focal+	Patchy+	–	1	Resection	NO	AWD	60
7	Congenital	M	Leg	*MCC-BRAF*	–	–	+	–	1	MEK inhibitor	NO	AWD	11
8	1 month	M	Leg	*AGAP3-BRAF*	+	–	–	–	1	MEK inhibitor, MEK/mTOR inhibitor combo	NO	AWD	8
9	3 months	M	Paraspinal	*KIAA1549-BRAF*	–	–	–	–	6	Resection	NO	NED	12
10	5 months	M	RP	*OSBP-BRAF*	–	–	–	–	44	Resection, adjuvant chemo	NO	NED	10
11	7 months	M	Arm	*DAAM1-BRAF*	–	–	–	–	1	Resection, adjuvant chemo	NO	NED	24
12	15 years	M	Leg	*TEX41-BRAF*	Patchy+	–	+	UNK	1	Resection	NO	NED	12
13	18 years	F	Anterior mediastinum	*NRF1-BRAF*	Patchy+	–	UNK	Focal cyto+	1	UNK	NO	AWD	3
14	32 years	M	RP	*FOXN3-BRAF, TRIP11-BRAF*	–	–	–	UNK	10	Resection, adjuvant chemo, BRAF/MEK inhibitor combo	YES	DOD	9

IHC immunohistochemistry, *Mits* mitoses per 10 high power field, *Mets* metastasis, *mo* months, *M* male, *F* female, *cCMN* cellular congenital mesoblastic nephroma, *RP* retroperitoneum, *N/A* not applicable, *IUFD* intrauterine fetal demine, *WGA* weeks gestational age, *AWD* alive with disease, *NED* no evidence of disease, *DOD* dead of disease, *UNK* unknown, *TBD* to be determined, *combo* combination therapy, *cyto* cytoplasmic.

[a]Contained three alternative splice variants of the *EPB41L2-BRAF* fusion.

performed on all cases, with assay specifics varying by institution. Cases 1, 2, 5, 6, 9, and 12 were investigated using the UW-OncoPlex Cancer Gene Panel, a targeted DNA capture-based NGS assay performed on Illumina NextSeq500 and/or HiSeq2500 systems (Illumina, San Diego, CA, USA) [23]. Case 3 was evaluated using the UCSF500 Cancer Gene Panel, a custom hybrid-capture NGS assay performed on the HiSeq2500 (Illumina) platform [24]. A custom anchored multiplex amplicon-based panel from Boston Children's Hospital performed on Illumina MiSeq was used to investigate Cases 7 and 8 [25]. Cases 4, 6, 10, and 13 were studied using FusionPlex (ArcherDX, Boulder, CO, USA), an anchored multiplex RNA sequencing assay performed on HiSeq2000 systems (Illumina) [25]. Cases 11 and 14 were evaluated with GeneTrails Comprehensive Solid Tumor Panel, a combined DNA and RNA amplicon-based NGS assay performed on the NextSeq500/550 (Illumina) platforms [26, 27].

Fluorescence in situ hybridization

Interphase FISH was performed on unstained FFPE tissue sections or touch imprint slides. FISH using dual-color, break-apart probes annealed to the *ETV6* gene region [*ETV6* (*TEL*) (12p13); Vysis, Inc., cat. #07J77-001] was performed on Cases 1–3, 5, and 11.

Analysis

Fisher's exact test was used to evaluate relationships between molecular alteration, morphologic pattern, immunoprofile, mitotic rate, metastasis, and survival. The size of the data set was too limited for evaluation of site predilection, stage at diagnosis, or logarithmic analysis of mitotic activity.

Results

BRAF point mutations as novel drivers for spindle cell sarcomas within the spectrum of IFS

BRAF-activating point mutations were present in five cases (Cases 1–5), including both index cases (see Fig. 1A). The tumor from Case 1 contained a previously described Ras-independent activating (Class 2) *BRAF* point mutation (p.L485F) located within the *BRAF* tyrosine kinase domain [28]. Case 2 contained a *BRAF* p.V600D mutation, which has not previously been described in soft tissue tumors, but is similar to the more common tumorigenic *BRAF* p.V600E mutation (present in Cases 3–5). Point mutations involving codon 600 are so-called Class I *BRAF* mutations and result in Ras-independent (constitutive) monomeric action of

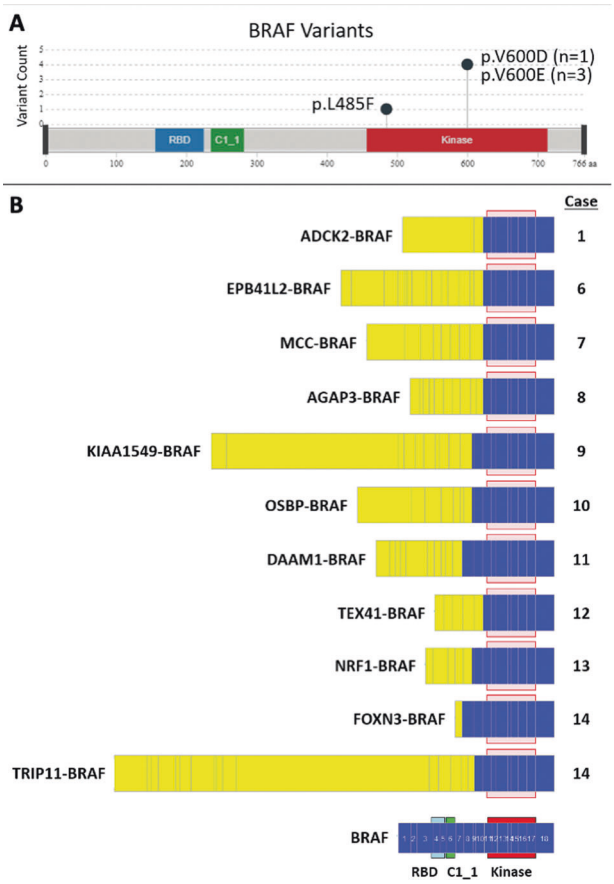

Fig. 1 Molecular alterations. A Five tumors demonstrated *BRAF* point mutations, including p.L485F (Case 1), p.V600D (Case 2), and p.V600E (Cases 3–5). **B** Ten tumors (Cases 1, 6–14) demonstrated *BRAF* rearrangements including fusion of the *BRAF* kinase domain to various partners.

BRAF [21, 29]. No additional pathologic genetic alterations were detected in any of these five cases bearing *BRAF* point mutations, with the exception of Case 1 that additionally contained a *BRAF* gene fusion.

Multiple novel BRAF fusions identified in spindle cells sarcomas within the spectrum of IFS-like tumors

Targeted sequencing of Case 1 and the remaining nine cases (6–14) revealed *BRAF* gene fusions (See Fig. 1B). The majority of the fusions (seven) were novel, including *BRAF-ADCK2*, *MCC-BRAF*, *OSBP-BRAF*, *DAAM1-BRAF*, *TEX41-BRAF*, *FOXN3-BRAF*, and *TRIP11-BRAF*. The *KIAA1549-BRAF* fusion in Case 9 has previously been described in gliomas [21, 30] and reported in one malignant phyllodes tumor [31] and one malignant spindle cell chest wall lesion in an adult [20]. The *NRF1-BRAF* fusion in Case 13 has been described in gliomas [32] and one urothelial carcinoma [33]. The fusions *EPB41L2-BRAF* and *AGAP3-*

BRAF have each been described once previously, in diffuse glioma [34] and melanoma [35], respectively. Of note, in this cohort, Case 6 contained three different *EPB41L2-BRAF* alternative splice variants with in-frame fusions of exons 12, 14, and 15 to the tyrosine kinase domain of *BRAF*. In addition, Case 14 harbored two distinct *BRAF* fusions (*FOXN3-BRAF* and *TRIP11-BRAF*). Two cases contained additional genetic alterations: Case 1, as mentioned above with a *BRAF* p.L485F and Case 14 that additionally contained a *MUTYH* p.G396D substitution.

Clinicopathologic features

The clinicopathologic features are summarized in Table 1. Patients presented at a median age of 6 months (range: congenital to 32 years) with 9/14 (64%) presenting within the first year of life and 3/14 (21%) of cases presenting congenitally. Only one patient was over 18 years of age, at age 32 years (Case 14). The tumors exhibited a male predilection (2.5:1). The most common clinical history, when available, was a "rapidly" growing mass. Tumors were otherwise identified via physical exam or imaging, as in the congenital cases.

Tumors occurred in the extremities ($n = 5$, 36%), axial sites ($n = 3$), head and neck ($n = 2$) retroperitoneum ($n = 2$), and visceral locations ($n = 2$). One of the visceral tumors (Case 5) arose in the kidney and was therefore classified as cCMN (Case 5).

Morphology

Morphologically, the tumors exhibited a variety of histologic patterns, including ovoid to short spindle cells arranged in intersecting fascicles (11/13) (Fig. 2A) and/or haphazardly (9/13) (Fig. 2B). Branching ectatic/"HPC-like" vessels were often present (7/13) (Fig. 2C, D). Cellularity ranged from markedly cellular to relatively hypocellular (Fig. 2A, D, E, respectively). Infiltrative growth was present in all cases (Fig. 2E, F). In one case the primary morphologic pattern was infiltrative growth into adipose tissue reminiscent of "lipofibromatosis" (Case 8); other cases showed this pattern at the periphery but this was not the primary/central morphologic pattern (Fig. 2E, F). Perivascular and stromal hyaline deposition were each noted twice, occurring in a total of three cases (Fig. 2G); five tumors demonstrated myxoid stroma (Fig. 2B). Ten tumors were associated with a chronic inflammatory infiltrate. Additional features included "inflammatory myofibroblastic tumor-like," myoid-like, and biphasic patterns, seen in four, two, and two cases, respectively. Often tumors showed intratumoral heterogeneity, with multiple patterns in a single case. A single paraspinal based tumor (Case 1) contained heterologous cartilage (Fig. 2H). The renal tumor was composed of spindle cells arranged in fascicles with scattered mitoses (3/10 hpf) (Fig. 2I); no concentric growth around entrapped tubules, juxtaglomerular cell hyperplasia, angiodysplasia, or metaplastic cartilage, or glial elements were present. Therefore, the morphology of this tumor was consistent with cCMN rather than metanephric stromal tumor. Mitoses ranged from 1 to 44 mitoses per 10 high power fields (median 1/10 hpf). One case contained focal necrosis, occupying <15% of the tumor (Case 1). No histologic feature demonstrated statistical significance with regard to molecular alteration (Fisher's exact test, $p > 0.5$).

Immunohistochemistry

The tumors demonstrated a nonspecific immunoprofile with variable staining for CD34, S100, and SMA (Fig. 3 and Table 1). Weak cytoplasmic expression of Pan-Trk was present in one case (Case 13; Fig. 3I), in the absence of *NTRK*-alterations. No marker demonstrated statistically significant association with regard to molecular alteration (Fisher's exact test, $p > 0.5$).

Outcome

Follow-up information was available for 12/14 cases, with length of follow-up ranging from 3 months to 5 years (median 11.5 months); two patients were lost to follow-up (Table 1). Of the 12 patients, 4 are alive with disease (33%), 6 are alive with no evidence of disease (54.5%), and 2 (16%) died of disease. Those who died of disease include Case 1, described above, which resulted in an IUFD at a gestational age of 29 weeks, and Case 14, wherein a 32-year-old man with an unresectable retroperitoneal tumor and lung metastases at the time of presentation progressed despite chemotherapy (including cycles of doxorubicin/ifosfamide, gemcitabine/paclitaxel, pazopanib, and combined BRAF/MEK inhibition with dabrafenib/trametinib) and who died 9 months after diagnosis due to hemorrhagic complications from brain metastases. Two other patients (Cases 7 and 8) received neoadjuvant targeted therapy in attempt to reduce surgical morbidity. In Case 7, MEK inhibitor (trametinib) monotherapy was given with subsequent decrease in tumor size, resolution of the patient's varus deformity, and resumption of ambulation; the patient is currently off therapy with stable disease for 6 months. In Case 8, the patient's disease progressed through trametinib monotherapy; however, disease stabilization occurred with combination trametinib/sirolimus therapy (MEK/mTOR inhibition). Both patients are currently alive with disease at 11 and 8 months, respectively. Only one patient (Case 14) experienced metastatic disease. Molecular alteration, histologic pattern, mitotic activity, and immunoprofile each did not demonstrate statistical significance with

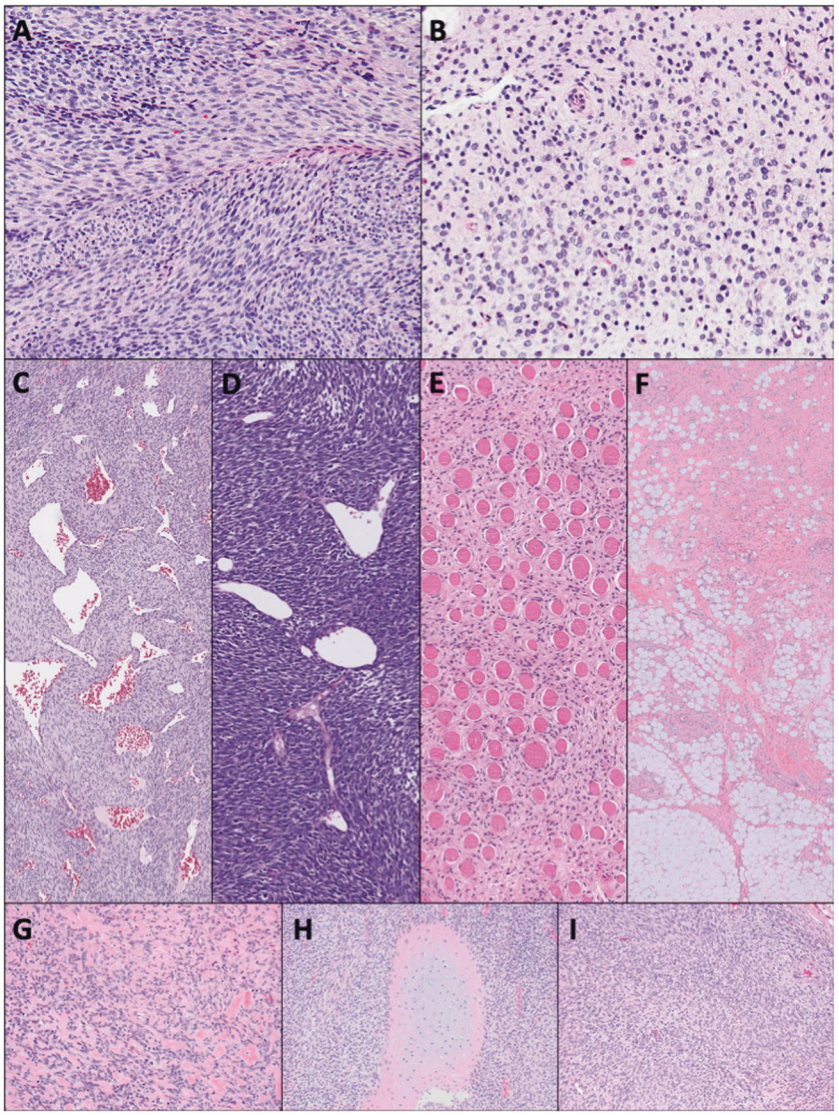

Fig. 2 Histologic features of *BRAF* gene-altered tumors. Tumors most commonly showed ovoid to spindle cells arranged in fascicles (**A**, Case 9) or haphazardly (**B**, Case 4) in either a collagenized or myxoid stroma. Most cases showed dilated ectatic/"HPC-like" vessels (**C**, Case 2 and **D**, Case 10). All tumors showed focal to marked infiltrative growth (**E**, Case 11), which often was most pronounced at the periphery of the mass as seen in Case 4 (**F**) where the primary mass was cellular with marked infiltration in the peritumoral adipose tissue. A subset of cases demonstrated either prominent stromal and/or perivascular hyalinization (**G**, Case 6). One case showed heterologous cartilaginous differentiation (**H**, Case 1). The cCMN showed diffuse cellular spindle cells arranged in fascicles (**I**, Case 5).

regard to presence of metastasis or survival (Fisher's exact test, $p > 0.5$).

Discussion

We evaluated a cohort of 14 patients with *BRAF*-altered spindle cell sarcomas morphologically overlapping with IFS. The patients were predominantly infants with only one patient over the age of 18 years; the median age was 6 months. A bimodal age distribution was observed with the larger peak in early infancy and a second peak in adolescents/young adults. A male predilection was seen. Histologically the tumors were composed of undifferentiated spindled to ovoid cells most frequently arranged haphazardly or in intersecting fascicles, often with HPC-like vasculature and/or a chronic inflammatory infiltrate; no specific immunophenotype was present. Our group expands a prior cohort of five cases of *BRAF* fusions in tumors overlapping with IFS and helps improve our understanding of these tumors [16], including adding seven novel *BRAF* fusions and for the first time *BRAF* point mutations as likely oncogenic drivers in these spindle cell sarcomas. The presence of both activating point mutations and fusions resulting in the same clinicopathologic phenotype reinforces the need for broad molecular profiling within this category of tumors.

Activating *BRAF* mutations, via fusion or point mutation, have been demonstrated as an oncogenic driver in a wide range of tumors, including thyroid carcinoma, melanoma, and gliomas [20, 21, 30–38]. However, *BRAF* gene alterations are uncommon in mesenchymal tumors. *BRAF* p.V600E, the most common *BRAF* alteration, has been documented in subset of both gastrointestinal stromal tumors (GIST) [39] and glomus tumors [40], and *BRAF* fusions are present in some myxoinflammatory fibroblastic

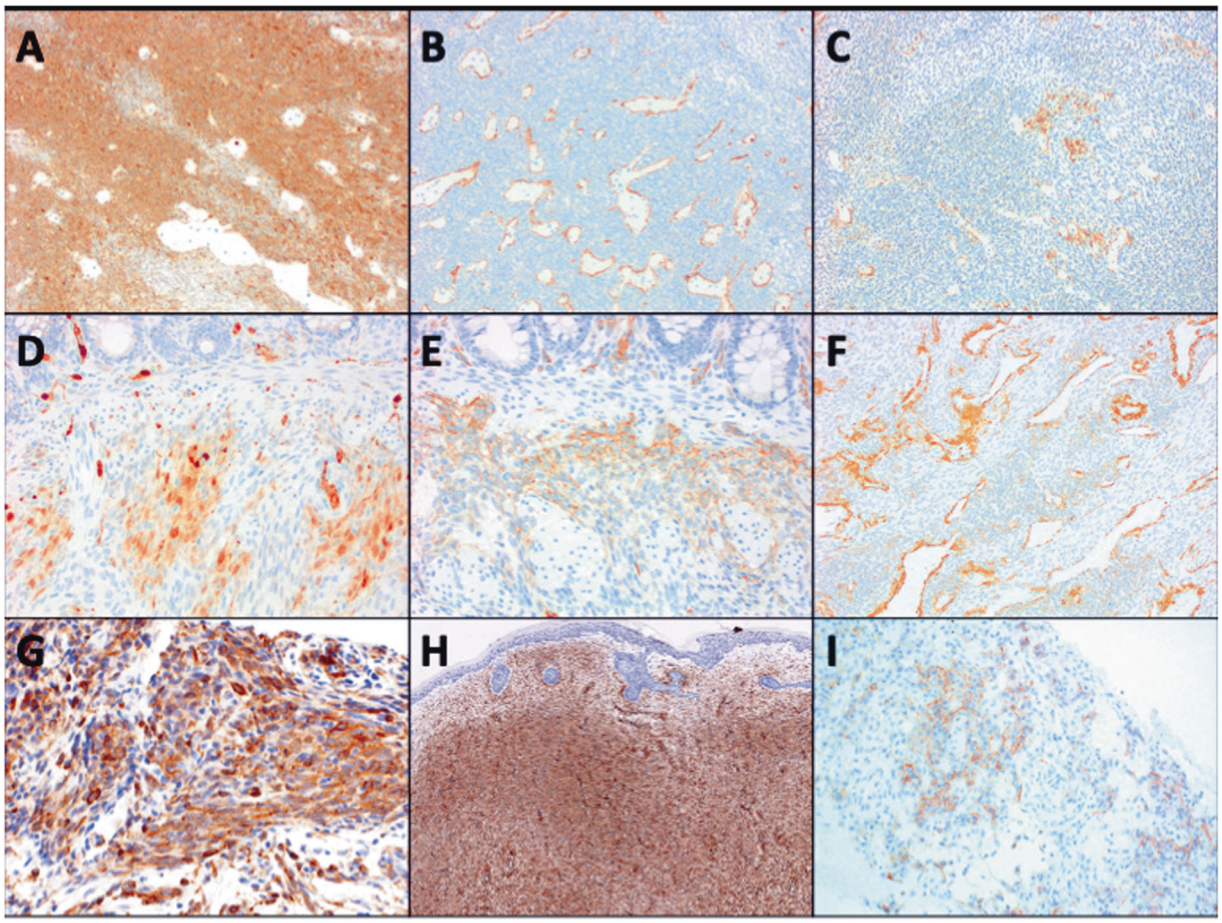

Fig. 3 Immunohistochemistry in *BRAF* gene-altered tumors. A subset of tumors demonstrated variable expression of CD34, S100, and SMA in tumor cells, while some cases showed no expression for any marker (Table 1). Example cases: Case 1 (**A**–**C**) **A** Diffuse S100 expression. **B** No CD34 expression; positivity in endothelial cells only. **C** Focal SMA expression. Case 2 (**D**–**F**). **D** Patchy S100 expression. **E** Patchy CD34 expression. **F** No SMA in tumor cells; SMA expression in pericytic cells only. **G** Case 7 showed strong SMA expression (without CD34 or S100, not pictured here) and **H** Case 3 showed diffuse strong expression of CD34 (without S100 expression, not pictured here). **I** Case 13 was the only case with patchy cytoplasmic Pan-Trk expression.

sarcomas (MIFS) [41]. Glomus tumors and MIFS entities are histologically distinct from the spindle cell tumors described herein, highlighting the need for morphologic and molecular correlation, whereas GIST could share histologic overlap with the BRAF-altered spindle cell sarcomas in this current series; however, immunophenotypically GIST differ, being distinguished by expression of CD117 and/or DOG1. In addition, *BRAF* p.V600E alterations are also present in metanephric tumors of the kidney (metanephric adenoma, adenofibroma, and stromal tumors) [42–44]; *NTRK* gene rearrangements have also been rarely described in epithelial metanephric adenomas [44]. However, whereas metanephric adenomas and adenofibromas contain primitive metanephric tubular/epithelial elements, metanephric stromal tumor does not and therefore could be in the differential diagnosis with CMN (classic or cellular subtypes). Histologic differences typically can distinguish metanephric stromal tumor and CMN, with metanephric stromal tumor often demonstrating concentric "onion-skinning" of spindle cells around entrapped tubules, heterologous glial or cartilaginous differentiation, and/or vascular changes (angiodysplasia, juxtoglomerular cell hyperplasia of entrapped glomeruli, entrapped arterioles) [45]. These features were not seen in the kidney tumor in this study; instead, this neoplasm was composed of relatively monomorphic cellular spindle cells arranged in fascicles, most in keeping with a diagnosis of cCMN.

Relatively limited data are present detailing *BRAF* alterations in spindle cell sarcomas, including those with clinicopathologic features overlapping with IFS/CMN (summarized in Table 1). A prior series examining genetic alterations in *ETV6-NTRK3*-negative undifferentiated spindle cell sarcomas with morphologic overlap with IFS identified five *BRAF* fusions as well as variant *NTRK* gene fusions [16]. Similarly, a study investigating both CMN and IFS lacking the canonical *ETV6-NTRK3* fusion identified

multiple oncogenic rearrangements in the MAPK signaling cascade, including *BRAF*-internal deletions (compound deletion and tandem duplication) and one *BRAF* gene fusion [15]. Of note, two of the IFS cases within the Wegert et al. study contained concurrent *ETV6-NTRK3* fusions and *BRAF*-internal deletions [15]; no data were available to determine if this represented tumor heterogeneity. Similarly, in the current study, one tumor contained multiple *BRAF* fusions (Case 14) and another (Case 1) contained both a *BRAF* point mutation and *BRAF* fusion; again, further investigation is required to determine whether these represent one or multiple clones. Both of the prior series examining *BRAF* spindle cell sarcomas were confined to pediatric patients, with no clinical follow-up [15, 16]. In the adult population, only three patients have previously been reported with spindle cell tumors harboring *BRAF* fusions [20, 46].

The prior cases of spindle cell sarcomas with *BRAF* alteration have reported variable expression of CD34 and S100, ranging from diffuse to focal expression [20, 46]. Variable expression of CD34 and/or S100 as well as SMA was observed in a subset of our cases (Fig. 3), with the case arising in an adult patient being negative for all of these markers. Of note, similar variability in CD34 and S100 expression profiles have been reported in tumors containing *NTRK* gene fusions as well as those with *MET*, *RET*, and *RAF1* gene fusions [8, 12–14, 47–50]. Some of these tumors have been reported to have IFS-like morphology [8, 11–16] and others to have "lipofibromatosis-like" morphology [45–47]; overlapping clinicodemographic and outcome data are reported. While this is the largest series of *BRAF*-altered spindle cell sarcomas, it still has a limited number of cases and more data are required to determine if particular morphologic features and/or immunohistochemical expression profiles are of prognostic significance.

Classically, IFS/CMN harbors *NTRK* gene rearrangements, most commonly *ETV6-NTRK3*. *NTRK1/2/3* genes encode for tropomyosin receptor kinases that signal through three primary signaling pathways, one of which is the RAS/MAPK/ERK pathway [51]. Therefore, the constitutive activation of *NTRK* signaling secondary to in-frame fusions of *NTRK* genes leads predictably to upregulation of the RAS/MAPK/ERK pathway [51]. BRAF is a serine-threonine kinase protein, belonging to the RAF (v-raf-1 murine leukemia viral oncogene homolog) family, comprising a series of serine/threonine-specific kinase effectors in the MAPK signaling pathway [29]. Activation of BRAF can occur via base substitutions (point mutations), the majority of which occur in the kinase domain, or via intact in-frame gene fusions of the *BRAF* kinase domain [29]. Both alterations lead to increased kinase activity, inducing the downstream phosphorylation of ERK protein and thus resulting in cell/tumor proliferation and survival. Alternative fusions described in in IFS-like tumors including *RET*, *MET*, and *RAF1 (CRAF)* [11–16] also signal through the RAS/MAPK/ERK pathway. Interestingly, this upregulation of the MAPK pathway and similar mRNA expression profiles are observed in tumors morphologically identified as IFS/CMN regardless of whether *ETV6-NTRK3* fusions are present, suggesting a possible biologic relationship between *NTRK* fusion-positive and -negative IFS/CMN [51]. As one would hypothesize, preliminary studies show that spindle cell tumors with *RAF1* gene fusions and IFS-like tumors with *BRAF* gene fusions cluster together by RNA unsupervised hierarchal cluster analysis, further supporting that they are related entities [46].

For this spectrum of tumors, the current World Health Organization (WHO) 5th Edition Classification of Soft Tissue and Bone Tumors includes both IFS and a provisional entity of "*NTRK*-rearranged spindle cell tumor" as diagnostic categories [52, 53]. The 5th Edition WHO presents updates from the prior 4th Edition classification regarding the pathogenesis of IFS, to include alternative genetic alterations outside the canonical *ETV6-NTRK3* gene fusion, including *NTRK1/2/3*, *MET*, *RET*, *RAF1*, and *BRAF* gene fusions. In addition, "NTRK-rearranged spindle cell tumor" was added as an emerging/provisional category of tumor, encompassing spindle cell tumors of variable morphologies, including "lipofibromatosis-like" and "peripheral nerve sheath-like" patterns with frequent CD34 and/or S100 expression. Similar genetic alterations to IFS are described as oncogenic drivers, including *NTRK1/2/3*, *RAF1*, and *BRAF* gene fusions [53]. As noted above, limited RNA profiling studies show overlap in these categories of tumors. Currently, it remains unclear if these two diagnostic categories represent one contiguous spectrum or multiple unique entities that can be separated by either morphology and/or genetics. Practically, nosology may be less important than identification of oncogenic genetic alterations with the potential to aid in diagnosis and treatment. As this study highlights, comprehensive molecular testing must cover both *BRAF* rearrangements and point mutations to identify all potentially oncogenic alterations. Important therapeutic decisions depend on the underlying means of BRAF activation [29]. V600 mutant tumors have shown good response to targeted BRAF inhibitors, such as vemurafenib and debrafenib [54, 55]; however, tumors with non-V600 point mutations and those harboring BRAF fusions have shown resistance to and/or paradoxical activation by these therapies [56, 57]. Targeted therapy for these tumors currently involves MEK inhibitors and/or duel MEK/BRAF inhibition [58, 59] and other treatment options, such as the so-called paradox-breaking and dimer-targeted RAF inhibitors, have shown promise in pre-clinical trials [56, 57, 60, 61]. However, evidence of BRAF alterations that remain resistant even to these second-generation

therapies is emerging [62], which underscores the importance of comprehensive molecular testing in order to match patients to the most effective therapy.

While our investigation did not uncover any correlation between tumor characteristics and outcome, our analysis is inherently limited due to the rarity of these tumors. Given the extensive overlap in the clinicopathologic features of *BRAF* alteration and *NTRK* fusion-driven IFS, we anticipate overlap in prognoses as well. However, studies of classic IFS and similar tumors have yet to identify reliable prognostic markers and we cannot predict how any individual tumor in this spectrum will behave. Therefore, accumulation of more cases remains imperative to enhance the classification of these tumors and ensure that patients are matched to the appropriate treatments.

In conclusion, we present the largest case series of *BRAF*-altered spindle cell sarcomas to date, significantly expanding the literature of these neoplasms. We report seven novel *BRAF* fusion partners, including one case with two concurrent *BRAF* fusions. We also report for the first time the existence of *BRAF* point mutations as likely oncogenic drivers in these tumors. Clinical demographics, histology, immunophenotype, and outcome data for our case series significantly overlap with the data published for *NTRK*-driven IFS.

Acknowledgements This study is part of a collaborative effort of Sarcoma Pediatric Pathology Research InTErest group (SPPRITEs).

Funding No funding was received for this study.

Compliance with ethical standards

Conflict of interest JLD has received fees for consulting and advisory board roles from Loxo Oncology/Bayer/Lilly Pharmaceuticals. The spouse of author CML is employed by Bayer Healthcare. All other authors declare no conflicts of interest and/or disclosures.

References

1. Stout AP. Fibrosarcoma in infants and children. Cancer. 1962;15:1028–40.
2. Chung EB, Enzinger FM. Infantile fibrosarcoma. Cancer. 1976;38:729–39.
3. Speleman F, Dal Cin P, De Potter K, Laureys G, Roels HJ, Leroy J, et al. Cytogenetic investigation of a case of congenital fibrosarcoma. Cancer Genet Cytogenet. 1989;39:21–24.
4. Mandahl N, Heim S, Rydholm A, Willen H, Mitelman F. Non-random numerical chromosome aberrations (+8, +11, +17, +20) in infantile fibrosarcoma (Letter). Cancer Genet Cytogenet. 1989;40:137–9.
5. Knezevich SR, Garnett MJ, Pysher TJ, Beckwith JB, Grundy PE, Sorensen PH. ETV6-NTRK3 gene fusions and Trisomy 11 establish a histologic link between mesoblastic nephroma and congenital fibrosarcoma. Cancer Res. 1998;58:5046–8.
6. Rubin BP, Chen CJ, Morgan TW, Xiao S, Grier HE, Kozakewich HP, et al. Congenital mesoblastic nephroma t(12;15) is associated with ETV6-NTRK3 gene fusion cytogenetic and molecular relationship to congenital (infantile) fibrosarcoma. Am J Pathol. 1998;153:1451–8.
7. Argani P, Fritsch MK, Shuster AE, Perlman EJ, Coffin CM. Reduced sensitivity of paraffin-based RT-PCR assays for ETV6-NTRK3 fusion transcripts in morphologically defined infantile fibrosarcoma. Am J Surg Pathol. 2001;25:1461–4.
8. Davis JL, Lockwood CM, Stohr B, Boecking C, Al-Ibraheemi A, DuBois SG, et al. Expanding the spectrum of pediatric NTRK-rearranged mesenchymal tumors. Am J Surg Pathol. 2019;43:435–45.
9. Church AJ, Calicchio ML, Nardi V, Skalova A, Pinto A, Dillon DA, et al. Recurrent EML4-NTRK3 fusions in infantile fibrosarcoma and congenital mesoblastic nephroma suggest a revised testing strategy. Mod Pathol. 2018;31:463–73.
10. Davis JL, Lockwood CM, Albert CM, Tsuchiya K, Hawkins DS, Rudzinski ER. Infantile NTRK-associated mesenchymal tumors. Pediatr Dev Pathol. 2018;21:68–78.
11. Coffin CM, Beadling C, Neff T, Corless CL, Davis JL. Infantile fibrosarcoma with a novel RAF1 rearrangement: The contemporary challenge of reconciling classic morphology with novel molecular genetics. Hum Pathol: Case Rep. 2020;22:200434.
12. Flucke U, van Noesel MM, Wijnen M, Zhang L, Chen CL, Sung YS, et al. TFG-MET fusion in an infantile spindle cell sarcoma with neural features. Genes Chromosomes Cancer. 2017;56:663–7.
13. Davis JL, Vargas SO, Rudzinski ER, Marti JML, Janeway K, Forrest S, et al. Recurrent RET gene fusions in paediatric spindle mesenchymal neoplasms. Histopathology. 2020;76:1032–41.
14. Antonescu CR, Dickson BC, Swanson D, Zhang L, Sung YS, Kao YC, et al. Spindle cell tumors with RET gene fusions exhibit a morphologic spectrum akin to tumors with NTRK gene fusions. Am J Surg Pathol. 2019;43:1384–91.
15. Wegert J, Vokuhl C, Collord G, Velasco-Herrera MDC, Farndon SJ, Guzzo C, et al. Recurrent intragenic rearrangement of EGFR and BRAF in soft tissue tumors of infants. Nat Commun. 2018;9:2378.
16. Kao YC, Fletcher CDM, Alaggio R, Wexler R, Zhang L, Sung YS, et al. Recurrent BRAF gene fusions in a subset of pediatric spindle cell sarcomas—expanding the genetic spectrum of tumors with overlapping features with infantile fibrosarcoma. Am J Surg Pathol. 2018;42:28–38.
17. Laetsch TW, DuBois SG, Mascarenhas L, Turpin B, Federman N, Albert CM, et al. Larotrectnib for paediatric solid tumours harbouring NTRK gene fusions: a multicentre, open-label, phase 1 study. Lancet Oncol. 2018;19:705–14.
18. Gupta A, Belsky JA, Schieffer KM, Leraas K, Varga E, McGrath SD, et al. Infantile fibrosarcoma-like tumor driven by novel RBPMS-MET fusion consolidated with cabozantinib. Cold Spring Harb Mol Case Stud. 2020;6:a005645.
19. Doebele RC, Davis LE, Aishnavi A, Le AT, Estrada-Bernal A, Keysar S, et al. An oncogenic NTRK fusion in a soft tissue sarcoma patient with response to the tropomyosin-related kinase (TRK) inhibitor LOXO-101. Cancer Disco. 2015;5:1049–57.
20. Subbiah V, Westin SN, Wang K, Araujo D, Wang WL, Miller VA, et al. Targeted therapy by combined inhibition of the RAF and mTOR kinases in malignant spindle cell neoplasm harboring the KIAA1549-BRAF fusion protein. J Hematol Oncol. 2014;7:8.
21. Schreck KC, Grossman SA, Pratilas CA. BRAF mutations and the utility of RAF and MEK inhibitors in primary brain tumors. Cancers (Basel). 2019;28:126.

22. Crotty EE, Leary SES, Geyer JR, Olson JM, Millard NE, Sato AA, et al. Children with DIPG and high-grade glioma treated with temozolomide, irinotecan, and bevacizumab: the Seattle Children's Hospital experience. J Neurooncol. 2020;148:607–17.
23. Kuo JA, Paulson VA, Hempelmann JA, Beightol M, Todhunter S, Colbert BG, et al. Validation and implementation of a modular targeted capture assay for the detection of clinically significant molecular oncology alterations. Practical Lab Med. 2020;19: e00153.
24. Kline CN, Joseph NM, Grenert JP, van Ziffle J, Talevich E, Onodera C, et al. Targeted next-generation sequencing of pediatric neuro-oncology patients improves diagnosis, identifies pathogenic germline mutations, and directs targeted therapy. Neuro Oncol. 2017;19:699–709.
25. Zheng Z, Liebers M, Zhelyazkova B, Cao Y, Panditi D, Lynch KD, et al. Anchored multiplex PCR for targeted next-generation sequencing. Nat Med. 2014;20:1479–84.
26. Beadling C, Neff TL, Heinrich MC, Rhodes K, Thornton M, Leamon J, et al. Combining highly multiplexed PCR with semiconductor-based sequencing for rapid cancer genotyping. J Mol Diagn. 2013;15:171–6.
27. Beadling C, Wald AI, Warrick A, Neff TL, Zhong S, Nikiforov YE, et al. A multiplexed amplicon approach for detecting gene fusions by next-generation sequencing. J Mol Diagn. 2016;18:165–75.
28. Yaeger R, Kotani D, Mondaca S, Parikh A, Bando H, Van Seventer E, et al. Response to anti-EGFR therapy in patients with BRAF non-V600 mutant metastatic colorectal cancer. Clin Cancer Res. 2019;25:7089–97.
29. Yaeger R, Corcoran RB. Targeting alterations in the RAF-MEK pathway. Cancer Disco. 2019;9:329–41.
30. Antonelli M, Badiali M, Moi L, Buttarelli FR, Baldi C, Massimino M, et al. KIAA1549:BRAF fusion gene in pediatric brain tumors of various histogenesis. Pediatr Blood Cancer. 2015;62:724–7.
31. Nozad S, Sheehan CE, Gay LM, Elvin JA, Vergilio JA, Suh J, et al. Comprehensive genomic profiling of malignant phyllodes tumors of the breast. Breast Cancer Res Treat. 2017;162:597–602.
32. Phillips JJ, Gong H, Chen K, Joseph NM, van Ziffle J, Jin LW, et al. Activating NRF1-BRAF and ATG7-RAF1 fusions in anaplastic pleomorphic xanthoastrocytoma without BRAF p.V600E mutation. Acta Neuropathol. 2016;132:757–60.
33. Isaacson AL, Guseva NV, Bossler AD, Ma D. Urothelial carcinoma with an NRF1-BRAF rearrangement and response to targeted therapy. Cold Spring Harb Mol Case Stud. 2019;5:a003848.
34. López G, Oberheim Bush NA, Berger MS, Perry A, Solomon DA. Diffuse non-midline glioma with H3F3A K27M mutation: a prognostic and treatment dilemma. Acta Neuropathol Commun. 2017;5:38.
35. Kulkarni A, Al-Hraishawi H, Simhadri S, Hirshfield KM, Chen S, Pine S, et al. BRAF fusion as a novel mechanism of acquired resistance to vemurafenib in BRAFV600E mutant melanoma. Clin Cancer Res. 2017;23:5631–8.
36. Xing M. Molecular pathogenesis and mechanisms of thyroid cancer. Nat Rev Cancer. 2013;13:184–99.
37. Hutchinson KE, Lipson D, Stephens PJ, Otto G, Lehmann BD, Lyle PL, et al. BRAF fusions define a distinct molecular subset of melanomas with potential sensitivity to MEK inhibition. Clin Cancer Res. 2013;19:6696–702.
38. Kaley T, Touat M, Subbiah V, Hollebecque A, Rodon J, Lockhart AC, et al. BRAF inhibition in BRAFV600-mutant gliomas: results from the VE-BASKET study. J Clin Oncol. 2018;36:3477–84.
39. Hostein I, Faur N, Primois C, Boury F, Denard J, Emile JF, et al. BRAF mutation status in gastrointestinal stromal tumors. Am J Clin Pathol. 2010;133:141–8.
40. Karamzadeh Dashti N, Bahrami A, Lee SJ, Jenkins SM, Rodriguez FJ, Folpe AL, et al. BRAF V600E mutations occur in a subset of glomus tumors, and are associated with malignant histologic characteristics. Am J Surg Pathol. 2017;41:1532–41.
41. Kao YC, Ranucci V, Zhang L, Sung YS, Athanasian EA, Swanson D, et al. Recurrent BRAF gene rearrangements in myxoinflammatory fibroblastic sarcomas, but not hemosiderotic fibrolipomatous tumors. Am J Surg Pathol. 2017;41:1456–65.
42. Choueiri TK, Cheville J, Palescandolo E, Fay AP, Kantoff PW, Atkins MB, et al. BRAF mutations in metanephric adenoma of the kidney. Eur Urol. 2012;62:917–22.
43. Argani P, Lee J, Netto GJ, Zheng G, Tseh-Lin M, Park BH. Frequent BRAF V600E mutations in metanephric stromal tumor. Am J Surg Pathol. 2016;40:719–22.
44. Catic A, Kurtovic-Kozaric A, Sophian A, Mazur L, Skenderi F, Hes O, et al. KANK1-NTRK3 fusions define a subset of BRAF mutation negative renal metanephric adenomas. BMC Med Genet. 2020;21:202.
45. Argani P, Beckwith JB. Metanephric stromal tumor. Am J Surg Pathol. 2000;24:917–26.
46. Suurmeijer AJH, Dickson BC, Swanson D, Zhang L, Sung YS, Cotzia P, et al. A novel group of spindle cell tumors defined by S100 and CD34 co-expression shows recurrent fusions involving RAF1, BRAF, and NTRK1/2 genes. Genes Chromosomes Cancer. 2018;57:611–21.
47. Agaram NP, Zhang L, Sung YS, Chen CL, Chung CT, Antonescu CR, et al. Recurrent NTRK1 gene fusions define a novel subset of locally aggressive lipofibromatosis-like neural tumors. Am J Surg Pathol. 2016;40:1407–16.
48. Kao YC, Suurmeijer AJH, Argani P, Dickson BC, Zhang L, Sung YS, et al. Soft tissue tumors characterized by a wide spectrum of kinase fusions share a lipofibromatosis-like neural tumor pattern. Genes Chromosomes Cancer. 2020;59:575–83.
49. Hicks JK, Henderson-Jackson E, Duggan J, Joyce DM, Brohl AS. Identification of a novel MTAP-RAF1 fusion in a soft tissue sarcoma. Diagn Pathol. 2018;13:77.
50. Michal M, Ptáková N, Martínek P, Gatalica Z, Kazakov DV, Michalová K, et al. S100 and CD34 positive spindle cell tumor with prominent perivascular hyalinization and a novel NCOA4-RET fusion. Genes Chromosomes Cancer. 2019;58:680–5.
51. Gadd S, Beezhold P, Jennings L, George D, Leuer K, Huang CC, et al. Mediators of receptor tyrosine kinase activation in infantile fibrosarcoma: a Children's Oncology Group study. J Pathol. 2012;228:119–30.
52. Davis JL, Antonescu CR, Bahrami A. Infantile fibrosarcoma. In: WHO Classification of Tumours Editorial Board, editor. WHO classification of tumours of soft tissue and bone. 5th ed. Lyon: IARC; 2020. p. 119–21.
53. Suurmeijer AJH, Antonescu CR. NTRK-rearranged spindle cell tumor (emerging). In: WHO Classification of Tumours Editorial Board, editor. WHO classification of tumours of soft tissue and bone. 5th ed. Lyon: IARC; 2020. p. 287–9.
54. Poulikakos PI, Zhang C, Bollag G, Shokat KM, Rosen N. RAF inhibitors transactivate RAF dimers and ERK signaling in cells with wild-type BRAF. Nature. 2010;18:427–430.
55. Nobre L, Zapotocky M, Ramaswamy V, Ryall S, Bennett J, Alderete D, et al. Outcomes of BRAF V600E pediatric gliomas treated with targeted BRAF inhibition. JCO Precis Oncol. 2020;4: PO.19.00298.
56. Yao Z, Torres NM, Tao A, Gao Y, Luo L, Li Q, et al. BRAF mutants evade ERK-dependent feedback by different mechanisms that determine their sensitivity to pharmacologic inhibition. Cancer Cell. 2015;28:370–83.
57. Sievert AJ, Lang SS, Boucher KL, Madsen PJ, Slaunwhite E, Choudhari N, et al. Paradoxical activation and RAF inhibitor

resistance of BRAF protein kinase fusions characterizing pediatric astrocytomas. Proc Natl Acad Sci USA. 2013;110:5957–62.
58. Selt F, Hohloch J, Hielscher T, Sahm F, Capper D, Korshunov A, et al. Establishment and application of a novel patient-derived KIAA1549:BRAF-driven pediatric pilocytic astrocytoma model for preclinical drug testing. Oncotarget. 2017;8:11460–79.
59. Broman KK, Dossett LA, Sun J, Eroglu Z, Zager JS. Update on BRAF and MEK inhibition for treatment of melanoma in metastatic, unresectable, and adjuvant settings. Expert Opin Drug Saf. 2019;18:381–92.
60. Zhang C, Spevak W, Zhang Y, Burton EA, Ma Y, Habets G, et al. RAF inhibitors that evade paradoxical MAPK pathway activation. Nature. 2015;526:583–6.
61. Yao Z, Gao Y, Su W, Yaeger R, Tao J, Na N, et al. RAF inhibitor PLX8394 selectively disrupts BRAF-dimers and RAS-independent BRAF mutant-driven signaling. Nat Med. 2019;25:284–91.
62. Jain P, Surrey LF, Straka J, Russo P, Womer R, Li MM, et al. BRAF fusions in pediatric histiocytic neoplasms define distinct therapeutic responsiveness to RAF paradox breakers. Pediatr Blood Cancer. 2021:e28933.